Received: 22 June 2020 | Revised: 27 August 2020 | Accepted: 20 September 2020

DOI: 10.1111/ajt.16334

ORIGINAL ARTICLE

AJT

Urine recirculation prolongs normothermic kidney perfusion via more optimal metabolic homeostasis—a proteomics study

Annemarie Weissenbacher[1] | Honglei Huang[1,2] | Tomas Surik[1] | Maria L. Lo Faro[1] | Rutger J. Ploeg[1] | Constantin C. Coussios[3] | Peter J. Friend[1] | Benedikt M. Kessler[2]

[1]Nuffield Department of Surgical Sciences, University of Oxford, Oxford, UK

[2]Target Discovery Institute, Nuffield Department of Medicine, University of Oxford, Oxford, UK

[3]Institute of Biomedical Engineering, Department of Engineering Science, University of Oxford, Oxford, UK

Correspondence
Annemarie Weissenbacher
Email: annemarie.weissenbacher@i-med.ac.at

Present address
Annemarie Weissenbacher, Annemarie Weissenbacher, Department of Visceral, Transplant and Thoracic Surgery, Medical University of Innsbruck, Innsbruck, Austria
Honglei Huang, Honglei Huang, Oxford BioMedica Plc, Oxford, UK

We describe a proteomics analysis to determine the molecular differences between normothermically perfused (normothermic machine perfusion, NMP) human kidneys with urine recirculation (URC) and urine replacement (UR). Proteins were extracted from 16 kidney biopsies with URC (n = 8 donors after brain death [DBD], *n* = 8 donors after circulatory death [DCD]) and three with UR (*n* = 2 DBD, *n* = 1 DCD), followed by quantitative analysis by mass spectrometry. Damage-associated molecular patterns (DAMPs) were decreased in kidney tissue after 6 hours NMP with URC, suggesting reduced inflammation. Vasoconstriction was also attenuated in kidneys with URC as angiotensinogen levels were reduced. Strikingly, kidneys became metabolically active during NMP, which could be enhanced and prolonged by URC. For instance, mitochondrial succinate dehydrogenase enzyme levels as well as carbonic anhydrase were enhanced with URC, contributing to pH stabilization. Levels of cytosolic and the mitochondrial phosphoenolpyruvate carboxykinase were elevated after 24 hours of NMP, more prevalent in DCD than DBD tissue. Key enzymes involved in glucose metabolism were also increased after 12 and 24 hours of NMP with URC, including mitochondrial malate dehydrogenase and glutamic-oxaloacetic transaminase, predominantly in DCD tissue. We conclude that NMP with URC permits prolonged preservation and revitalizes metabolism to possibly better cope with ischemia reperfusion injury in discarded kidneys.

KEYWORDS
ischemia reperfusion injury (IRI), kidney (allograft) function / dysfunction, kidney biology, kidney transplantation / nephrology, organ perfusion and preservation, translational research / science

1 | INTRODUCTION

Proteomic profiling by mass spectrometry (MS) can rapidly identify global protein changes in cells and tissues, providing insights into pathways and interaction networks.[1-3] MS has been widely used in medical research and in the field of transplantation, contributing to the knowledge of organ function and failure at a molecular level.[4-6] However, none of the numerous protein biomarkers, which have been described in the recent

Abbreviations: CIT, cold ischemia time; DBD, donation after brain death; DCD, donation after circulatory death; HMP, hypothermic machine perfusion; IRR, intrarenal resistance; NMP, normothermic machine perfusion; SCS, static cold storage; TPN, total parenteral nutrition; URC, urine recirculation; UR, urine replacement; WIT, warm ischemia time.

[Correction added on 11 December 2020, after first online publication: the author name 'Maria L. L. Faro' has been corrected to 'Maria L. Lo Faro'.]

literature, has been implemented in the clinical routine yet to provide specific diagnosis for a defined phenotype of kidney allograft disease.[6] Most of the available data on kidney proteomics are on the detection of acute kidney allograft rejection markers earlier than biopsy could prove it. For instance, interferon-gamma induced chemokines CXCL9 and CXCL10, recruiting T cells to inflammatory sites, are clinically the most promising urine protein biomarkers at present.[7,8] Kaisar et al described the ability of proteomic analysis on biopsies to differentiate between outcomes after deceased donor kidney transplantation. Their results suggested that the outcome-related protein abundance was strongly linked with profibrotic and antioxidative proteins as well as proteins involved in apoptosis,[9] also observed in transcriptomics studies.[7,8] Besides the desire to improve prediction of outcome and rejection after kidney transplantation using -omics, there is little available on the topic of ex vivo normothermic perfusion (NMP). The purpose of applying proteomics to NMP tissue samples was to determine the molecular effects of normothermically perfused discarded human kidneys.

In light of all the relevant circumstances necessary for developing a transportable normothermic kidney perfusion device, we analyzed and published URC in discarded human kidneys and in experimental porcine kidney work previously.[9-11] Urine recirculation (URC) should help to facilitate an automated stand-alone kidney NMP system which could be clinically applicable without the requirement to replace the excreted urine volume actively. Furthermore, URC enables stable hemodynamics, perfusate volume, and homeostasis.[9,10] Compared to urine replenishment with Ringer's lactate, it is possible to perfuse discarded human kidneys for up to 24 hours normothermically when the urine is recirculated.[9-11]

We aimed to profile kidney proteomes, which are biologically distinct from others, and explore the impact of URC to control perfusion homeostasis and perfusate volume. This was compared to biopsies taken from kidneys perfused with urine replacement (UR), using Ringer's lactate, as described by other research groups before.[12-15]

2 | METHODS

Human kidneys were recovered for the purpose of transplantation but deemed untransplantable during post-recovery assessment at the donor hospital or at the transplant center. After transport to Oxford, normothermic perfusions were performed at the Institute of Biomedical Engineering (IBME), University of Oxford.[16] Donor characteristics, warm (WIT) and cold ischemia times (CIT) and perfusion parameters were collated and analyzed. The study was evaluated and approved by the national ethics review committee of the United Kingdom (REC reference 12/EE/0273 IRAS project ID 106793).

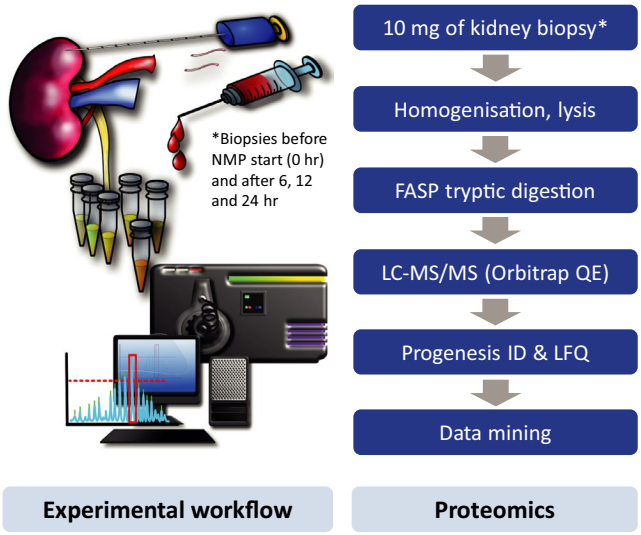

FIGURE 1 Kidney biopsy retrieval and proteomics workflows used in this study. Discarded kidneys were subjected to normothermic perfusion (NMP) either with urine recirculation (URC) or urine replacement (UR), and kidney cortex tissue biopsies collected at time points between 0 and 24 hours. Tissue material was homogenized, lysed, digested with trypsin using a filter-assisted sample preparation (FASP) protocol followed by liquid chromatography tandem mass spectrometry (LC-MS/MS) label-free quantitative analysis (LFQ) and data processing using MaxQuant and Perseus software

2.1 | Kidney biopsy preparation, protein extraction and digestion

Biopsies were taken at six different time points; zero biopsy at start of back table preparation, 1, 6, 12, 18, and 24 hours after perfusion start and at the end of perfusion, respectively. Core needle biopsy specimens, 18 gauge, were taken and stored at −80°C until use. The kidney biopsy retrieval protocol and −omics workflow are illustrated in Figure 1. Detailed description in Data S1.

2.2 | Protein identification and quantitation by mass spectrometry

Samples were analyzed using liquid chromatography tandem mass spectrometry (LC-MS/MS) as described previously.[17] In brief, a Dionex Ultimate 3000 nano-ultra performance liquid chromatography system coupled to an Orbitrap Fusion Lumos Tribrid Mass Spectrometer (Thermo Scientific) acquiring data in electron

FIGURE 2 NMP with URC or UR leads to different Kidney tissue proteomes. A. Volcano plot showing kidney proteomes of time zero URC versus UR biopsies. In red are proteins whose abundances were increased and in blue proteins with decreased abundance levels in URC T0 hours kidney tissues as compared to UR T0 hours. B. Volcano plot showing the proteome of kidneys subjected to 6 hours NMP either with URC or UR. In red are proteins whose abundances were increased, in blue proteins with decreased abundance levels in URC T6 hours kidney tissue as compared to UR T6 hours

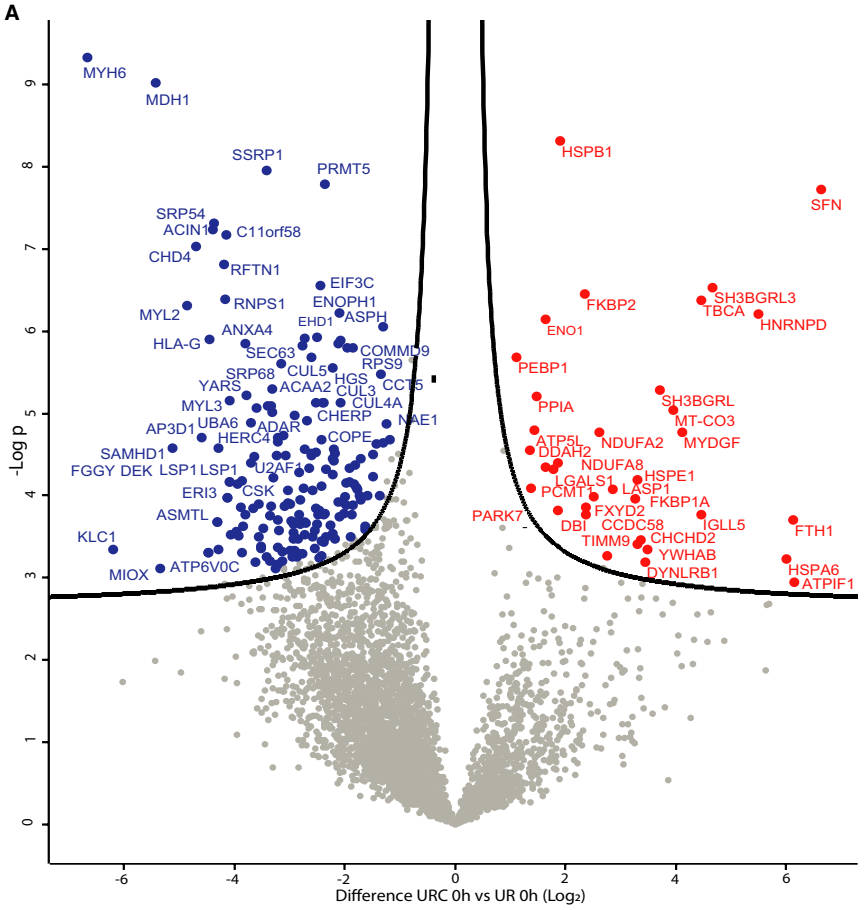
A
-Log p
Difference URC 0h vs UR 0h (Log2)
MYH6
MDH1
SSRP1
PRMT5
SRP54
ACIN1
C11orf58
CHD4
RFTN1
EIF3C
RNPS1
ENOPH1
MYL2
EHD1
ASPH
ANXA4
HLA-G
SEC63
COMMD9
RPS9
SRP68
CUL5
HGS
YARS
ACAA2
CUL3
CCT5
MYL3
CUL4A
CHERP
AP3D1
UBA6
ADAR
NAE1
HERC4
COPE
SAMHD1
FGGY
DEK
LSP1
U2AF1
ERI3
CSK
ASMTL
KLC1
MIOX
ATP6V0C
HSPB1
SFN
FKBP2
SH3BGRL3
TBCA
HNRNPD
ENO1
PEBP1
PPIA
SH3BGRL
MT-CO3
ATP5L
NDUFA2
MYDGF
DDAH2
NDUFA8
LGALS1
HSPE1
PCMT1
LASP1
FKBP1A
PARK7
FXYD2
DBI
CCDC58
IGLL5
FTH1
TIMM9
CHCHD2
YWHAB
DYNLRB1
HSPA6
ATPIF1

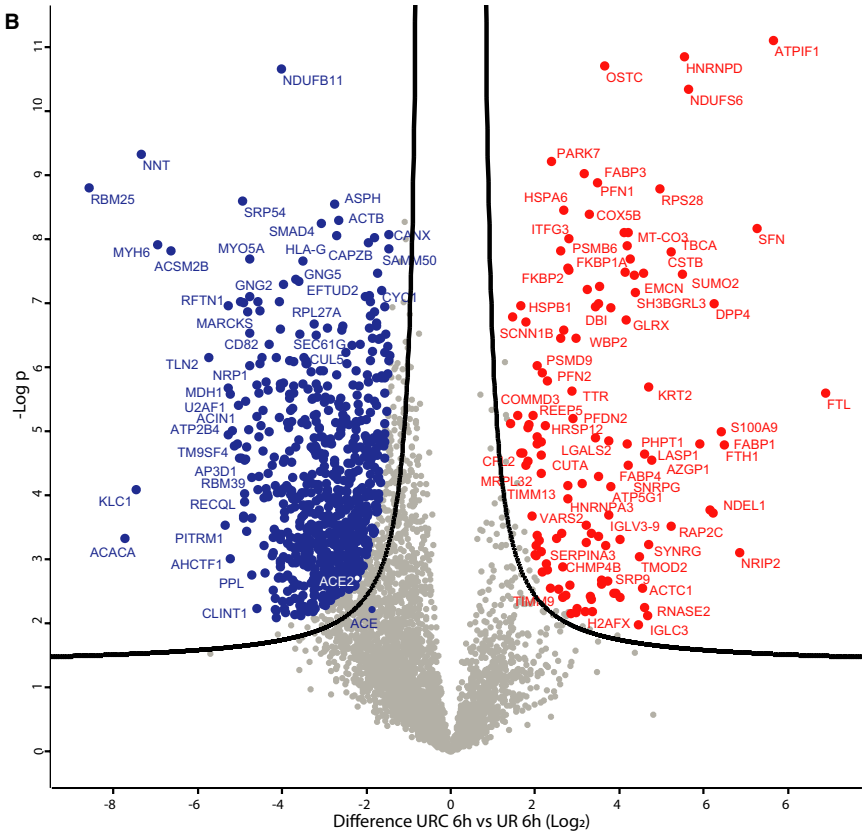
B
-Log p
Difference URC 6h vs UR 6h (Log2)
NDUFB11
NNT
RBM25
SRP54
ASPH
ACTB
SMAD4
CANX
MYH6
MYO5A
HLA-G
CAPZB
SAMM50
ACSM2B
GNG5
GNG2
EFTUD2
CYC1
RFTN1
RPL27A
MARCKS
CD82
SEC61G
CUL5
TLN2
NRP1
MDH1
U2AF1
ACIN1
ATP2B4
TM9SF4
AP3D1
RBM39
KLC1
RECQL
PITRM1
ACACA
AHCTF1
PPL
CLINT1
ACE2
ACE
ATPIF1
OSTC
HNRNPD
NDUFS6
PARK7
FABP3
PFN1
RPS28
HSPA6
COX5B
ITFG3
MT-CO3
TBCA
SFN
PSMB6
FKBP1A
CSTB
FKBP2
SUMO2
EMCN
HSPB1
SH3BGRL3
DPP4
DBI
GLRX
SCNN1B
WBP2
PSMD9
PFN2
KRT2
FTL
COMMD3
TTR
REEP5
PFDN2
HRSP12
S100A9
PHPT1
FABP1
LGALS2
LASP1
FTH1
CFL2
CUTA
AZGP1
FABP4
MRPL32
SNRPG
TIMM13
ATP5G1
NDEL1
HNRNPA3
VARS2
IGLV3-9
RAP2C
SERPINA3
SYNRG
NRIP2
CHMP4B
TMOD2
SRP9
ACTC1
TIMP1
RNASE2
H2AFX
IGLC3

TABLE 1 Kidneys undergoing proteomics after normothermic machine perfusion

Kidneys with urine recirculation (URC)												
Overall (n = 16)	Age in years	Sex	GFR[a] (ml/min/1.73 m^2)	Hypertension	DBD (n = 8)	DCD (n = 8)	Reason for discard	CIT in hours	CIT >24 hours	NMP time in hours	Median arterial flow in ml/min	Lactate @6 hours NMP in mmol/l	Urine in ml/hour
Kidney 1	70	male	59	no		X	patchy perfusion	15.0		16.2	330	14.1	86.3
Kidney 2	61	male	92	no	X		esophageal cancer	19.1		24.3	330	15.1	41.0
Kidney 3	70	male	125	no		X	patchy perfusion	32.0	X	12.3	410	19.9	3.3
Kidney 4	58	male	118	no	X		huge cyst lower pole	10.4		18.6	330	2.6	20.0
Kidney 5	73	male	45	yes	X		patchy perfusion	20.7		24.1	250	19.3	5.8
Kidney 6	51	female	70	no		X	renal neoplasia	11.4		24.2	320	12.9	44.9
Kidney 7	48	male	232	no		X	patchy perfusion, long CIT	51.2	X	15.0	250	20.0	111.8
Kidney 8	44	female	100	no		X	patchy perfusion, long CIT	36.1	X	24.1	305	11.2	16.7
Kidney 9	44	female	92	no		X	patchy perfusion, cortical necrosis	104.1	X	24.0	325	17.2	11.0
Kidney 10	49	male	178	no		X	patchy perfusion	25.3	X	24.3	510	10.6	25.4
Kidney 11	67	female	63	no	X		patchy perfusion	18.5		24.0	260	13.4	17.2
Kidney 12	38	male	58	yes		X	suspicion of pancreatic cancer	29.2	X	24.4	365	15.1	26.3
Kidney 13	68	male	101	no	X		patchy perfusion	108.1	X	24.0	514	6.6	6.5
Kidney 14	70	female	119	yes	X		stenosis of renal artery	17.5		24.1	413	8.2	53.5
Kidney 15	47	female	29	no	X		vascular damage, patchy perfusion	12.7		24.1	230	20.0	471.9
Kidney 16	76	female	152	yes	X		long CIT	15.4		24.0	787	5.6	51.0
Kidneys without urine recirculation (UR)													
Overall (n = 3)	**Age in years**	**Sex**	**GFR[a] (ml/min/1.73 m^2)**	**Hypertension**	**DBD (n = 2)**	**DCD (n = 1)**	**Reason for discard**	**CIT in hours**	**CIT >24 hours**	**NMP time in hours**	**Median arterial flow in ml/min**	**Lactate @6 hours NMP in mmol/l**	**Urine in ml/hour**
Kidney 17	74	female	90	yes		X	lesion on partner kidney	22.0		6.2	486	4.5	74.2
Kidney 18	78	female	61	yes	X		vascular damage	18.4		9.4	100	19.7	102.2
Kidney 19	71	female	77	no	X		organ size	21.1		8.2	371	17.8	84.4

Abbreviations: DBD, donation after brain death; DCD, donation after circulatory death; CIT, cold ischemia time; MP, normothermic machine perfusion.

[a]MDRD (modification of diet in renal disease) GFR (glomerular filtration rate) calculator.

spray ionization (ESI) positive mode was used with a 75-µm-inner diameter x 50 cm C18 EASY-Spray column (2 µm particle size, Thermofisher Scientific, United Kingdom). Peptides were separated with a 60 minutes gradient of 0% solvent A to 40% solvent B (solvent A: 99.9% H_2O, 0.1% formic acid, 5% DMSO; solvent B: 94.9% ACN, 0.1% formic acid, 5% DMSO) at 250 nl/min. MS survey acquisition was set with a resolution of 120 000 FWHM with a recording window between 400 and 1500 m/z. A maximum of 20 MS/MS scans were triggered in data-dependent acquisition (DDA) mode.

2.3 | Proteomics data analysis

Protein identification. Raw LC-MS/MS data were uploaded to Andromeda/Maxquant version 1.5.2.8 for MS/MS spectra matching against complete human data set (UPR_HumanSapiens, retrieved at 15/02/2017, 92 954 entries) with trypsin specificity.[18] Two missed cleavages, NQ deamination and methionine oxidation were selected as variable modification, carbamidomethylation of cysteine was selected as fixed modification. For identification, the FDR (false discovery rate) at the peptide spectrum matches (PSM) and protein level were set to 0.01. Unmodified unique+razor peptides were chosen for label-free quantification (LFQ) with minute ratio count set as 2. Match between run was selected to increased number of proteins with quantitative value. PANTHER classification system was used to perform gene ontology enrichment analysis (over represented or under represented). KEGG (Kyoto Encyclopaedia of Genes and Genomes) was used for canonical pathway assignment and STRING (v 11.0) for visualization.

The mass spectrometry proteomics data have been deposited to the ProteomeXchange Consortium via the PRIDE partner repository with the dataset identifier PXD021507.

Quantitative analysis. Quantitative MS data were uploaded to the Perseus software package (v1.5.5.3)[19] for data visualization and statistical analysis. Label-free quantitation (LFQ) values were first log2 transformed, then plotted in histograms to check normality of the data. Scatter plot display was used to display data in Figure 3. Hierarchical clustering analysis and heat maps were used to group samples based on the abundance of identified proteins after Z-score normalization and subtraction of mean values across columns (Figure S2). Two-sample t tests combined with Permutation FDR to correct for multiple testing were applied to detected differentially expressed proteins between comparisons. Statistical FDR set as 0.05, s0 as 0.1 in the volcano plot used to visualize differentially expressed proteins in Figure 2.

2.4 | Western blot validation of differentially expressed proteins

Twenty microgram of homogenized renal cortex proteins was denatured at 95°C for 5 minutes in Laemmli buffer and loaded onto 4%-12% pre-cast SDS-PAGE gels (Bio-Rad). Detailed description in Data S1.

2.5 | Statistical analysis

For statistical evaluation of the data (excluding proteomics), unpaired t tests (parametric) and Mann–Whitney tests (nonparametric) were performed using GraphPad Prism 7. Correlation analysis was performed using IBM SPSS Statistics Version 23. A value of $P < 0.05$ was considered significant.

3 | RESULTS

Overall, biopsies of 19 kidneys were analyzed using an optimized proteomics workflow (Figure 1). Protein was extracted from 16 kidneys with URC ($n = 8$ organs from brain dead donors [DBD], $n = 8$ from donors after circulatory death [DCD]), and three with UR ($n = 2$ DBD, $n = 1$ DCD). The mean cold ischemia time (CIT) for kidneys perfused with URC was 32.8 ± 30.6 hours (median 19.9 [10.4-108] hours); the mean warm ischemia time (WIT) was 18.5 ± 8.3 minutes. For the UR group, mean CIT was 20.5 ± 1.9 hours (median 21.1 [18.4-22] hours) and the only DCD in this group had 11 minutes WIT. The mean arterial flow of URC kidneys was 370 ± 139.5 ml/min; corresponding mean intrarenal resistance (IRR) was 0.27 ± 0.08 mmHg/ml/min. Kidneys perfused with UR had a mean arterial flow of 319 ± 198.2 ml/min; their mean IRR was 0.44 ± 0.4 mmHg/ml/min. Table 1 displays donor and kidney demographics. Kidney parenchyma did not deteriorate over time in any of the perfused organs. Table S3 shows histology and KIM-1 immunohistochemistry results, the tubular condition, of kidneys before perfusion start and at the end of NMP.

Urine recirculation achieved a stabilization of urine flow, which was not observed for kidneys under UR (Figure S1). The perfusion protocol appears to have global effects on total kidney tissue proteomes, separating the overall profiles of URC and UR kidneys, whereas separations of DCD versus DBD and lengths of CIT were less prominent (Figure S2). Different protein abundance profiles were visualized in groups stratified for perfusion types: URC versus UR. Figure 2A-B illustrates the comparison of URC and UR kidneys. These volcano plots revealed significant differences already between protein abundance in the zero biopsies, as compared to the analysis performed after 6 hours of NMP. For instance, enzymes involved in energy metabolism such as ATP synthase (ATPF1), NADH dehydrogenase (NDUFS6), and oligosaccharyltransferase (OSTC), are emerging in the profiles of URC kidneys after 6 hours NMP (Figure 2B). To examine the differences between perfusion conditions at an individual kidney level, scatter plots of kidneys 14-16 (URC) and 17-19 (UR) were generated (Figure 3A-F). We observed considerable variation between kidneys but noted also even more profound changes beyond 6 hours of NMP with URC, reflecting a revitalization of metabolism, in

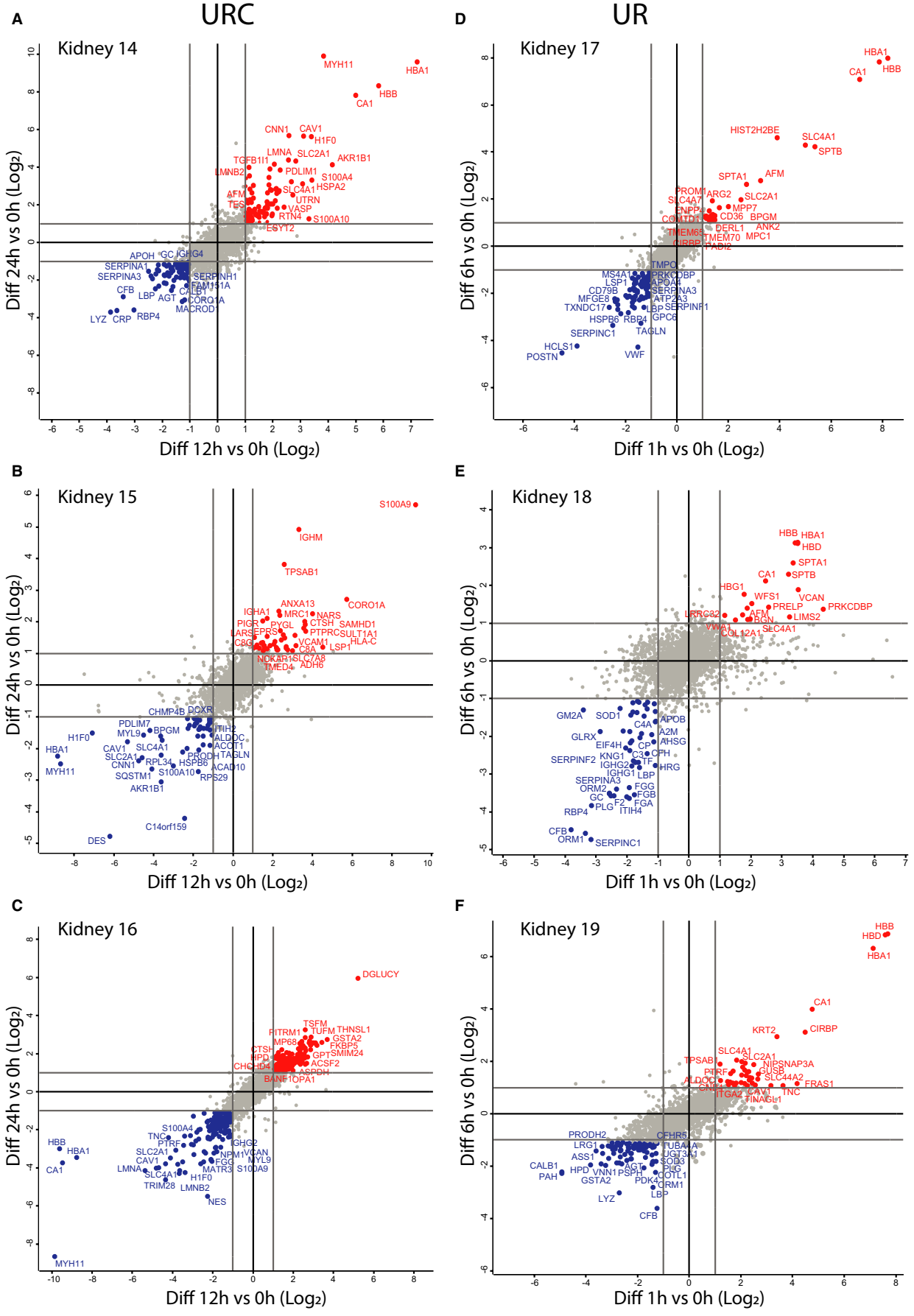
A
URC
Kidney 14
Diff 24h vs 0h (Log2)
Diff 12h vs 0h (Log2)
B
Kidney 15
Diff 24h vs 0h (Log2)
Diff 12h vs 0h (Log2)
C
Kidney 16
Diff 24h vs 0h (Log2)
Diff 12h vs 0h (Log2)
D
UR
Kidney 17
Diff 6h vs 0h (Log2)
Diff 1h vs 0h (Log2)
E
Kidney 18
Diff 6h vs 0h (Log2)
Diff 1h vs 0h (Log2)
F
Kidney 19
Diff 6h vs 0h (Log2)
Diff 1h vs 0h (Log2)

particular energy homeostasis. Perhaps not unexpectedly, kidney tissue proteome profiles at NMP and URC endpoints (beyond 6 up to 24 hours) were distinct from NMP and UR (6 hours).

3.1 | Enzymes involved in glucose and succinate metabolism increased after URC

Due to the fact that all NMP kidneys became metabolically active and consumed a different amount of glucose, in particular beyond the 6-hour time point, we first analyzed results specifically for proteins involved in glucose metabolism to discover potential differences in their up- and/or downregulation.

The comparison of biopsy samples from kidneys with a long CIT (>24 hours; kidneys 3, 7-10, 12, and 13; Table 1) with kidneys normothermically perfused after a shorter CIT (<24 hours; kidneys 1 and 2, 4-6, 11, 14-16; Table 1) revealed that the following enzymes stayed twofold, or less, downregulated throughout the time of perfusion (albeit not significantly) in the longer CIT cohort: glycolysis enzymes hexokinase (HK), phosphofructokinase (PFK) and pyruvate kinase (PK), glucose-6-phosphatase (G6P), fructose-1,6-bisphosphatase (FBP), phosphoenolpyruvate carboxykinase (PCK) and pyruvate carboxylase (PC), the key enzymes of gluconeogenesis.

When stratifying the proteomics analysis for donor type, DCD (n = 8) versus DBD (n = 8) URC kidneys, we could detect interesting trends of all mentioned enzymes involved in glucose metabolism, including mitochondrial malate dehydrogenase (MDH) and glutamic-oxaloacetic transaminase (GOT). All stated enzymes above were downregulated in the DCD zero biopsies compared to the DBD zero biopsies; FBP isoenzyme 1 was significantly (P< 0.05) downregulated in DCD kidneys compared to DBD organs. After 12 and 24 hours of NMP, all but one enzyme were more upregulated in DCD tissue compared to DBD kidney biopsies. The mitochondrial version of PCK, PCK2, was significantly downregulated (P < 0.05) after 12 hours of NMP in DCD kidney biopsies compared to DBD. Interestingly, both the cytosolic (PCK1) and the mitochondrial (PCK2) enzyme were more upregulated after 24 hours of NMP in DCD as compared to DBD tissue.

In DCD kidneys, succinate dehydrogenase (SDH; subunits A and B) were significantly upregulated in the zero biopsies as compared to DBD kidneys. After 12 and 24 hours of NMP the same proteins were significantly upregulated in DCD biopsies. Fumarate hydratase (FH), an enzyme which can reversibly catalyze the hydration/dehydration of fumarate to malate, was also significantly upregulated in the zero biopsies of DCD kidneys as compared to DBD tissue and vice versa after 12 hours of NMP.

3.2 | Proteins with altered abundance in kidney NMP with URC or UR

Damage-associated molecular pattern (DAMPs) proteins, known to be contributing to ischemia reperfusion injury (IRI), were significantly downregulated after 6 hours of kidney NMP and URC as compared to NMP and UR (Figure 3, Table S1).

Furthermore, the abundance of mitochondrial proteins such as d-glutamate cyclase (DGLUCY)[20] and succinate dehydrogenase subunits were significantly altered in URC biopsies, which could play a role regarding succinate accumulation and ROS production[21]: FH (fumarate hydratase), SDHB (succinate dehydrogenase complex, subunit B), SDHC (succinate dehydrogenase complex, subunit C), SDHD (succinate dehydrogenase complex, subunit D) (Figure 3A-C vs. D-F).

Kidneys perfused with URC expressed significantly more SLC4A1, a band 3 anion transport protein, which acts as a chloride/bicarbonate exchanger and is able to maintain the correct acid levels (pH) in the body. Furthermore, this protein mediates the chloride–bicarbonate exchange in the kidney which is required for normal acidification of the urine.[1-3]

Generally, protein profiles in kidneys with URC were exactly the opposite to the ones without, independent of their statistical significance. Figure 4A-D displays the comparison of up- and downregulated proteins with and without urine recirculation, emphasizing the four most striking clusters of metabolic activity: (1) acid–base balance and pH stability, (2) glucose metabolism, (3) anti-inflammation, and (4) the renin–angiotensin system.

Angiotensinogen (AGT) was upregulated in kidneys with UR and downregulated in kidneys with URC. Angiotensin I converting enzyme (ACE) was significantly downregulated in kidneys with URC, and serpin peptidase inhibitor (SERPINA3) was significantly upregulated in kidneys with URC after 6 hours (Figures 3 and 4), contributing to stabilizing urine flow rates during prolonged NMP (Figure S1).[1-3]

Carbonic anhydrase (CA1) was downregulated in kidneys with UR.[1-3,23] In kidneys perfused with URC it was possible to maintain physiological pH values throughout the perfusion period without giving any supplements. In kidneys without urine recirculation, UR group, the pH changed significantly over time in both directions—alkalotic and acidotic.

3.3 | Correlation of proteins with perfusion and organ characteristics

Several correlations were found between proteins of kidneys perfused with URC and UR with perfusion parameters (e.g. arterial flow, URC, blood gases, NMP time) and kidney factors (e.g. donor age) (Table S2).

FIGURE 3 NMP with URC or UR affects kidney proteome dynamics over time. Kidneys were subjected to NMP either with URC for 12 and 24 hours (A-C) or with UR for 1 and 6 hours (D-F), followed by quantitative proteomics analysis. Scatter plots show 24 hours/0 hours (y-axis) versus 12 hours/0 hours (X-axis) abundant ratios (A-C, for URC kidneys) or 6 hours/0 hours (y-axis) versus 1 hours/0 hours (X-axis) abundant ratios (D-F, for UR kidneys). Proteins elevated over NMP time are labeled in red, whereas proteins with reduced levels are highlighted in blue

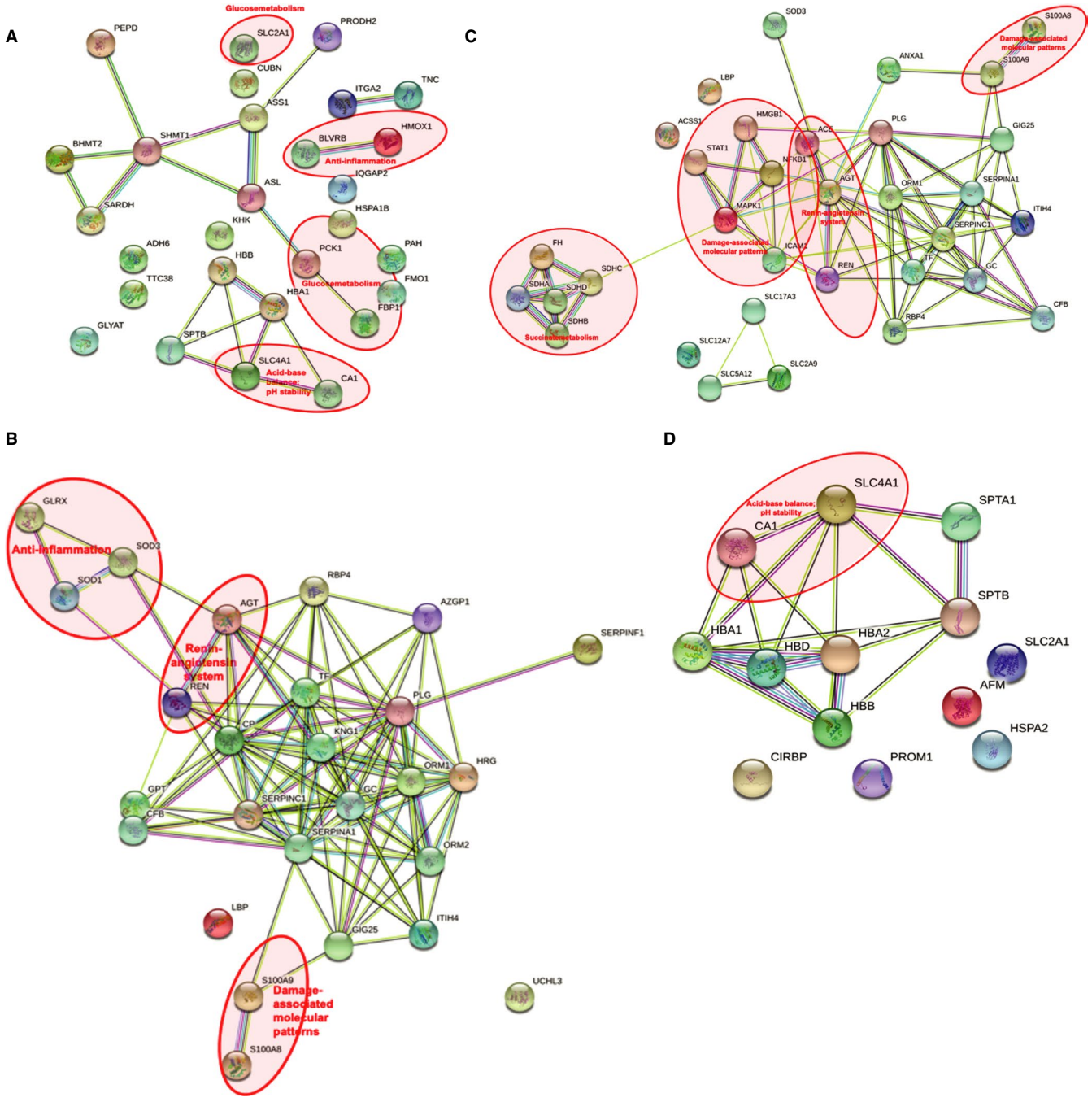

3.4 | NMP- and URC-dependent prolonged induction of enzymes contributing to metabolic homeostasis

In normothermically perfused kidneys with URC, proteins differentially expressed included antioxidants, stress proteins, anion exchangers, and enzymes like anhydrases and carboxykinases. We selected seven upregulated proteins in the group of kidneys with urine recirculation and validated the abundance profiles of these proteins by performing Western Blots on kidney tissue material. These included ICAM-1, SLC4A1 (band 3 anion transport protein), HMOX1 (hem oxygenase 1), flavin reductase (NADPH, gene BLVRB), CA1, PCK, and HSPA4 (Figure 5A-G). The signal intensity was quantified and normalized to beta-actin (Figure 6A-G). The number of selected proteins was limited by the available biopsy material. Strikingly, most effects were noticeable beyond 6 hours NMP. For instance, ICAM-1 increased significantly over time, reaching its peak 16 hours after perfusion start. Similarly, SLC4A1 and HMOX1 increased significantly from zero biopsy up to 18-24 hours after NMP initiation. BLVRB reached its peak 16 hours after NMP start compared to the zero biopsy. PCK got expressed throughout the perfusion without

any significant differences, the lowest amount of protein could be detected in biopsies taken 16 hours after NMP start; CA1 changed most significantly within the first 6 hours of NMP, followed by an additional increase in the time frame between 12 and 18 hours after NMP start; HSPA4 did not show significant changes between time points after NMP start. We conclude that prolonged NMP (>6 hours), facilitated by URC, permits a more effective metabolic homeostasis.

4 | DISCUSSION

Proteomics technology was applied to uncover the molecular profiles of kidney biopsies after NMP up to 24 hours, facilitated by urine recirculation (URC). Remarkably, prolonged NMP (>6 hours), not readily achievable without urine recirculation (UR), resulted in a more optimal metabolic homeostasis and showed signs of tissue damage recovery. For instance, we detected the downregulation of potential markers promoting ischemia reperfusion injury (IRI) during and after kidney NMP on a fully closed circuit by recirculating the urine. The aim of our series of normothermic perfusions was rather focusing on the development of a clinically applicable perfusion device for kidneys and to learn about and to understand processes going on during NMP. Therefore, we have not used whole blood to reperfuse NMP kidneys after a certain time of preservation mimicking IRI in the preclinical experimental setting.

Recirculation of the urine has been applied to a non-transplant model of kidney NMP up to 24 hours by our group before.[9,10] Volume control and balanced perfusate homeostasis as well as the possibility to have a fully automated and transportable kidney perfusion device, represent the three main advantages of URC in kidney NMP.[9,10] Generally, normothermic organ preservation has been an emerging field for the last two decades. Kidney NMP has been implemented as a clinical tool in the United Kingdom not only to reduce delayed graft function rates but also to enlarge the donor pool by rescuing discarded kidneys.[12,13,24-26] Several transplant centers around the globe have reported their first experiences with short-term kidney NMP (up to 1 to 2 hours) in the clinical setting, but with

FIGURE 4 Prolonged NMP with URC drives metabolic homeostasis. (A) Upregulated cellular pathways after 6 hours NMP with URC. Acid–base balance and pH stability: CA1 carbonic anhydrase 1; SLC4A1 band 3 anion transport protein. Glucose metabolism: PCK1 phosphoenolpyruvate carboxykinase; FBP1 fructose-1,6-bisphosphatase 1; SLC2A1 solute carrier family 2, facilitated glucose transporter member 1. Anti-inflammation: BLVRB flavin reductase (NADPH); broad specificity oxidoreductase that catalyzes the NADPH-dependent reduction of a variety of flavins, such as riboflavin, FAD or FMN, biliverdins, methemoglobin and PQQ (pyrroloquinoline quinone); contributes to heme catabolism and metabolizes linear tetrapyrroles; can also reduce the complexed Fe(3+) iron to Fe(2+) in the presence of FMN and NADPH. HMOX1 heme oxygenase 1; cleaves the heme ring at the alpha methene bridge to form biliverdin; biliverdin is subsequently converted to bilirubin by biliverdin reductase; exhibits cytoprotective effects since excess of free heme sensitizes cells to undergo apoptosis. (B) Upregulated cellular pathways after 6 hours NMP with UR. Renin–angiotensin system: AGT angiotensinogen; a potent regulator of blood pressure, body fluid, and electrolyte homeostasis. REN renin; to generate angiotensin I from angiotensinogen in the plasma, initiating a cascade of reactions that produce an elevation of blood pressure and increased sodium retention by the kidney. Damage-associated molecular patterns (DAMPs): S100A8 protein S100-A8; a calcium- and zinc-binding protein which plays a prominent role in the regulation of inflammatory processes and immune response. It can induce neutrophil chemotaxis and adhesion. Predominantly found as calprotectin (S100A8/A9) which has a wide plethora of intra- and extracellular functions. S100A9 protein S100-A9; a calcium- and zinc-binding protein which plays a prominent role in the regulation of inflammatory processes and immune response. It can induce neutrophil chemotaxis, adhesion, can increase the bactericidal activity of neutrophils by promoting phagocytosis via activation of SYK, PI3 K/AKT, and ERK1/2 and can induce degranulation of neutrophils by a MAPK-dependent mechanism. Anti-inflammation: GLRX glutaredoxin 1; has a glutathione-disulfide oxidoreductase activity in the presence of NADPH and glutathione reductase. SOD1 superoxide dismutase; destroys radicals which are normally produced within the cells and which are toxic to biological systems. SOD3 extracellular superoxide dismutase; protects the extracellular space from toxic effect of reactive oxygen intermediates by converting superoxide radicals into hydrogen peroxide and oxygen. (C) Downregulated cellular pathways after 6 hours NMP with URC. Renin–angiotensin system: AGT angiotensinogen; ACE angiotensin-converting enzyme; converts angiotensin I to angiotensin II by release of the terminal His-Leu, this results in an increase in the vasoconstrictor activity of angiotensin. Also able to inactivate bradykinin, a potent vasodilator. Damage-associated molecular patterns (DAMPs): HMGB1 high-mobility group box 1; promotes host inflammatory response to sterile and infectious signals and is involved in the coordination and integration of innate and adaptive immune responses. NFKB1 nuclear factor NF-kappa-B p105; a pleiotropic transcription factor; related to many biological processes such as inflammation, immunity, differentiation, cell growth, tumorigenesis, and apoptosis. MAPK1 mitogen-activated protein kinase 1; serine/threonine kinase which acts as an essential component of the MAP kinase signal transduction pathway. ICAM1 intercellular adhesion molecule 1; ligands for the leukocyte adhesion protein LFA-1 (integrin alpha-L/beta-2). STAT1 signal transducer and activator of transcription 1-alpha/beta; signal transducer and transcription activator that mediates cellular responses to interferons (IFNs), cytokine KITLG/SCF and other cytokines and other growth factors. S100A8 protein S100-A8. Succinate metabolism: SDHA/B/C/D succinate dehydrogenase subunits; A= flavoprotein subunit; B= iron–sulfur protein subunit; C and D= membrane anchoring subunits; involved in complex II of the mitochondrial electron transport chain and is responsible for transferring electrons from succinate to ubiquinone (coenzyme Q). FH fumarate hydratase; class II fumarase/aspartate family. (D) Downregulated cellular pathways after 6 hours NMP with UR. Acid–base balance and pH stability: CA1 carbonic anhydrase 1; SLC4A1 band 3 anion transport protein. NMP=normothermic machine perfusion of the kidney. UR=urine replacement. URC=urine recirculation. String Version 11.0; © String Consortium 2020.[22] Lines: line color indicates the type of interaction evidence; Nodes: colored—query proteins and first shell of interactors; white—second shell of interactors; empty—proteins of unknown 3D structure; filled—some 3D structure is known or predicted

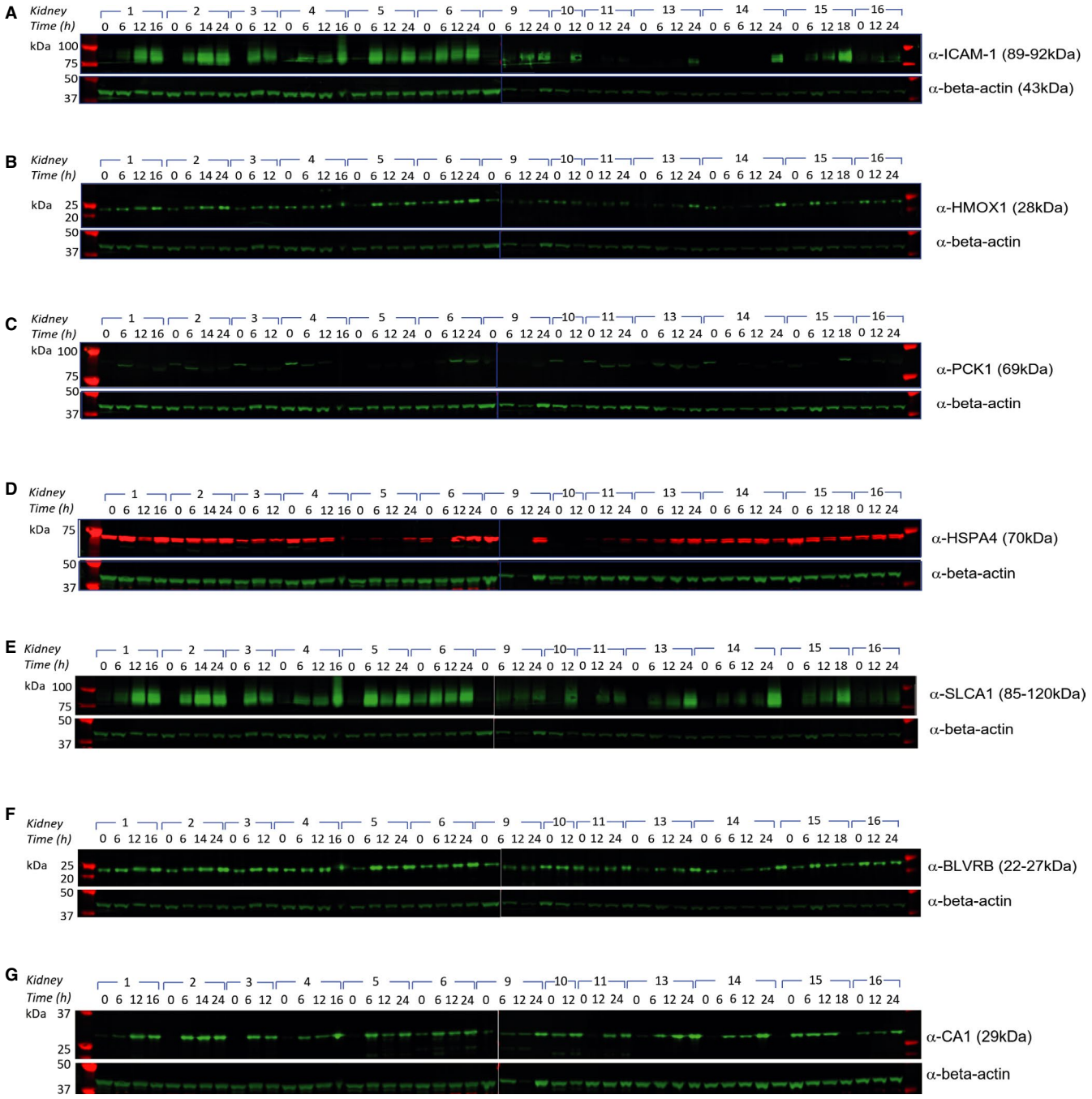

FIGURE 5 Altered protein profiles associated with prolonged NMP and URC. Western blotting of discarded kidney tissue extracts collected at different time points during NMP with URC: (A) α-ICAM-1, (B) α-HMOX1, (C) α-PCK1, (D) α-HSPA4, (E) α-SLC4A1, (F) α-BLVRB, (G) α-CA1. Beta-actin was used as loading control

the exception of the group around Nicholson et al publications are still missing. The first results of a prospective randomized trial comparing 1 hour NMP with static cold storage (SCS) in DCD kidneys is expected to be presented end of 2020.[13] Short-term kidney NMP appears to be quite common in the world of clinical transplantation, but long-term ex vivo kidney preservation going beyond 12 hours is still a subject of experimental work. Selzner et al are leading the field of porcine kidney perfusion, reaching overall preservation times of 24 hours.[14,15,27-29] In their recent publication, they describe the clear superiority of porcine DCD grafts preserved normothermically over grafts preserved by hypothermic perfusion or SCS in an auto-transplant model.[29] Although promising and clearly leading the way towards long-term kidney NMP, the necessity of replacing the lost urine volume in a perfusion system constitutes a limitation for a straightforward use in the clinical world.

In our perfusion system of kidney NMP up to 24 hours, we experienced the application of URC as extremely helpful, facilitating long-term NMP even after CIT beyond 50 hours without harming kidney parenchyma.[9,10] Keeping kidneys going normothermically by replacing excreted urine 1:1 using Ringer's lactate,

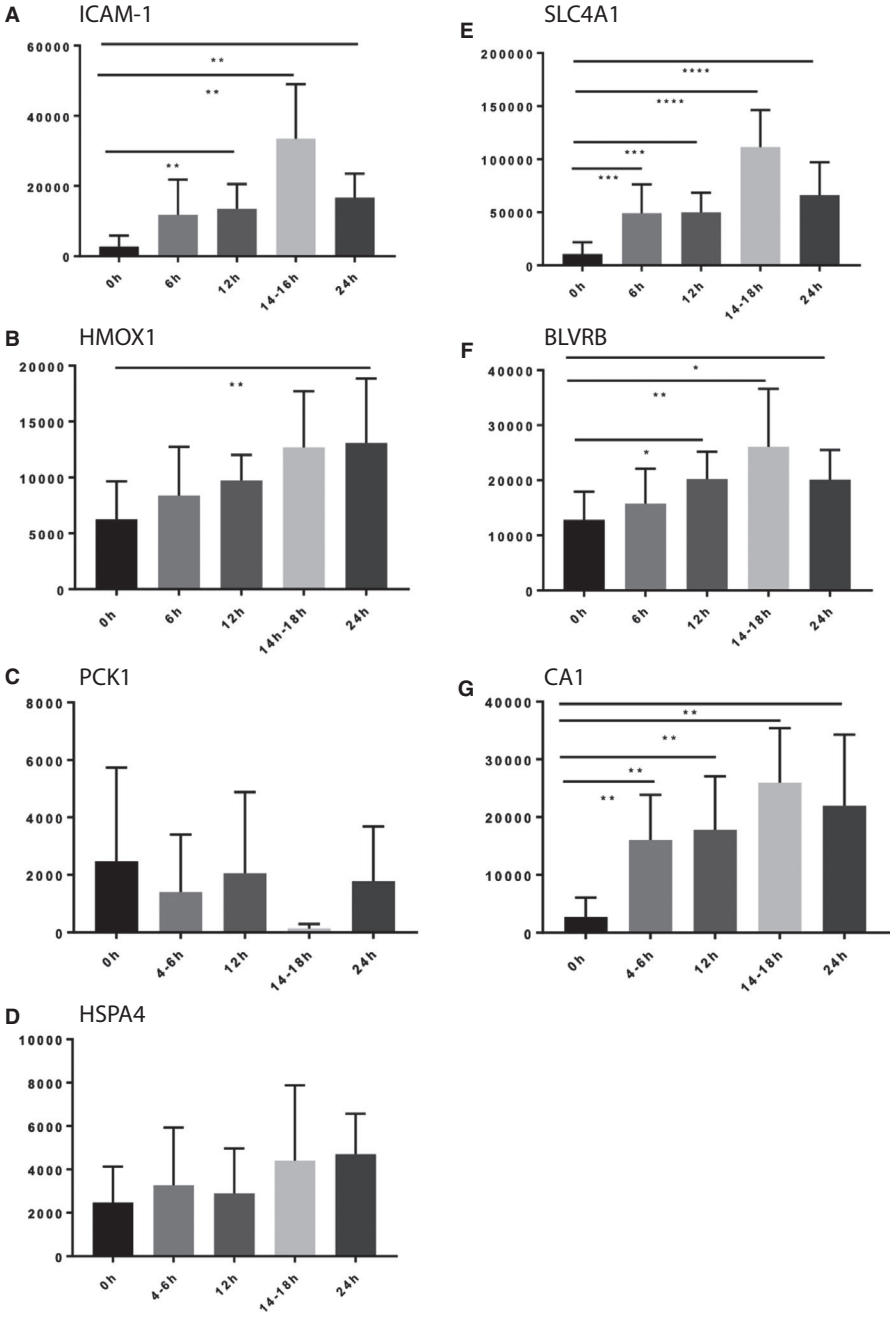

FIGURE 6 Prolonged NMP leads to increased levels of proteins contributing to metabolic *homeostasis*. Bar graphs show quantitative levels of proteins at times zero (0 hours), 6 hours, 12 hours, 14 hours-18 hours, and 24 hours, respectively. Protein levels of ICAM-1 (A), HMOX1 (B), PCK1 (C), HSPA4 (D), SLC4A1 (E), BLVRB (F), and CA1 (G) derived from Western blotting analysis are shown, normalized to beta-actin

as demonstrated by other research groups, was not feasible in our setting and led to renal artery flows <50 ml/min after 6 to 8 hours of NMP and/or severely alkalotic or acidotic perfusate (Figures S1 and S3).[9,10] The heterogenous cohort of perfused discarded human kidneys in this study, which were deemed untransplantable by all transplant centers in the United Kingdom at the time and perfused after variable durations of SCS, were not considered for clinical transplantation, however, we wanted to investigate any differences and similarities on the protein level of such preserved organs. Despite the low number of NMP kidneys with UR, which demands cautious interpretation of statistical significance, the most striking findings were the extent of differences (Figure 2) and the complete reversed up- and downregulation of proteins in kidneys perfused with and without urine URC (Figure 3). In all kidneys perfused with UR the proteins extracted after 6 hours NMP, such as DAMPs, proteins involved in succinate metabolism and vasoconstriction, were all upregulated compared to kidneys perfused with URC (Table S1). DAMPs can be released by injured tissue or

activated cells, following a stimulus and are recognized by cellular receptors as a universal damage-associated molecular pattern, able to initiate repair, provoke remodeling and innate immune signaling.[30] Reduction of DAMPs by using URC might not have an immediate impact on the kidney while being perfused on the circuit. However, it might cause less reperfusion injury when such kidneys are reperfused in a potential organ recipient in future transplant studies. A similar explanation applies to downregulated proteins involved in the succinate metabolism after NMP with URC. Studies on ischemic tissue and reperfusion showed succinate accumulation as a consequence of IRI.[31,32] Chouchani et al described in an ischemic model of the heart that succinate accumulation is a metabolic signature of ischemia and is responsible for mitochondrial ROS production during reperfusion. Succinate accumulation is caused by reverse function of succinate dehydrogenase driven by fumarate overflow.[31] In our biopsies, several subunits of the succinate dehydrogenase complex were significantly downregulated after six NMP hours with URC as compared to UR. A hallmark of perfused kidneys with UR was the significant upregulation of proteins involved in vasoconstrictive processes when compared to kidneys perfused with URC. Angiotensinogen (AGT)[33] which was upregulated in kidneys with UR and downregulated in kidneys with URC, is an interesting target due to its function and the fact that kidneys with UR developed increasing intrarenal resistance during NMP, leading to a deterioration of the arterial flow from hour 6 onwards. Angiotensinogen is part of the renin–angiotensin system regulating blood pressure, fluid balance, and salts in the human body. Angiotensinogen is converted to angiotensin I, which is converted to angiotensin II, a vasoconstrictor.[17] In addition to this finding, the comparison of the entire biopsy cohort of kidneys with and without URC revealed significant differences in other proteins involved in the renin–angiotensin system: ACE was significantly downregulated in kidneys with URC. Serpin peptidase inhibitor (SERPINA3) can inhibit the conversion of angiotensin-1 to the active angiotensin-2 indirectly and was significantly upregulated in kidneys with URC after 6 hours (Figure 2B).[22,34,35] Moreover, sodium content of the perfusate changed over time. Perfusate of kidneys undergoing NMP with UR had significantly higher sodium levels with 159.6 ± 4.63 mmol/l[9] as compared to URC kidneys with physiological levels of 141.3 ± 2.71 mmol/l, $P < 0.01$. Hypernatremia is a well-known factor inducing vasoconstriction of renal vasculature, but if this is triggered in our cohort by different protein up- or downregulations induced by different ways of handling urine and perfusate volume, cannot be answered at the current stage of investigations.

Carbonic anhydrase (CA1) may also contribute to an increased performance of kidneys perfused with urine recirculation (URC), and was found to be downregulated in kidneys with UR. We were able to maintain physiological pH values throughout the perfusion period only in kidneys perfused with URC. In contrast, urine replacement, caused either acidosis or alkalosis of the perfusate in our experiments. This could be due to a lack of presence or activity of CA1.[22,34-36] The most important function of this enzyme is to maintain the acid–base balance in human blood and tissue. In addition, band 3 anion transport protein SLC4A1 was also significantly upregulated over time in kidneys perfused with URC (Figures 3,5,6). This protein is crucial to maintain the correct acid levels in the human body, mediated by the chloride–bicarbonate exchange in the kidney, and it is required for the normal acidification of the urine.[22,34,35]

The profile of enzymes involved in gluconeogenesis and glycolysis could also help to explain the difficulty to interpret lactate levels in kidney NMP, which is an easy task in liver NMP. In humans, lactate metabolism plays a major role in the native kidney and the renal cortex appears to be the most important lactate-consuming organ after the liver.[18] Bartlett et al showed years ago that renal dysfunction impacts lactate and glucose metabolism. It is most likely that lactate levels are related to active glucose metabolism, glycolysis, and gluconeogenesis in the kidney. Also, there seems to be a cortico-medullary glucose-lactate recycling system: the medulla consumes glucose by active glycolysis and generates lactate. The cortex has the ability to take up the lactate released by the medulla and uses it for oxidation and gluconeogenesis.[19] A publication by Hui et al demonstrated that glucose is essential in feeding the Krebs-cycle via circulating lactate.[37] In their experimental setting in mice they detected strongly labeled lactate in the kidney after infusion of ^{13}C-labeled glucose, although intermediates of the Krebs cycle were more labeled after lactate infusion. An explanation for this pattern in the kidney is the heterogeneity of kidney cells; the presence of glycolytic cells producing lactate from glucose and oxidative cells using lactate to make Krebs cycle intermediates.[37]

Having in mind that proteomics technology will not be able to instantly advise us on decision making to transplant or not to transplant a kidney or to reallocate an organ to a better-matching recipient, and was not developed for this purpose, it is still offering important information by providing protein profiles able to be correlated with perfusion, donor, and transplant characteristics. Interestingly, levels of CA1, SLC4A1, and Tenascin-C (TNC) increased in accordance with higher arterial flow through the kidneys. Tenascin-C was fairly recently reported to be protective against acute kidney injury (AKI).[38] In an ex vivo model of AKI TNC is induced at injured sites of the organ, recruits Wnt ligands and creates an optimal microenvironment for tubular repair and regeneration.[38] In addition, levels of SOD3 were lower the higher the arterial flow was. This underlines the importance of reaching high and physiological renal plasma flow and, moreover, should recommend arterial flow as one of the most essential perfusion characteristics to assess a kidney ex vivo. Catalase expression increased the longer the kidney was on the circuit with urine recirculation. As expected, ICAM-1 was elevated the higher the arterial pressure was, but considerably reduced the longer the kidney underwent NMP. FAM3C, which promotes epithelial to mesenchymal transition,[1-3] was significantly associated with donor age, CIT, and intrarenal resistance, but correlated inversely with the time on the NMP device. This would suggest FAM3C to have a positive effect of longer term kidney NMP on the epithelial structures and proposes the implementation of such technology in the clinical setting for extended criteria donor organs in particular.

In conclusion, proteomics applied on consecutively taken biopsies of NMP kidneys revealed clear differences between URC and UR. Ameliorated metabolic processes due to prolonged NMP and URC could lead to enhanced kidney organ function recovery and render kidneys more amenable to transplantation.

ACKNOWLEDGMENTS

Special thanks to Stefan Scheidl, MD, Department of Visceral, Transplant and Thoracic Surgery, Medical University of Innsbruck, Innsbruck, Austria, for designing, creating, and providing Figure 1. Honglei Huang, PhD, was supported by a National Institute of Health Research (NIHR) grant to Rutger J. Ploeg.

DISCLOSURE

The authors of this manuscript have conflicts of interest to disclose as described by the *American Journal of Transplantation*. In addition to being full-time academics at the University of Oxford, PJF and CCC receive consultancy payments as nonexecutive medical and technical directors of OrganOx Limited, and are shareholders.

OPEN RESEARCH BADGES

This article has earned an Open Data badge for making publicly available the digitally-shareable data necessary to reproduce the reported results. The data is available at http://proteomecentral.proteomexchange.org/cgi/GetDataset.

DATA AVAILABILITY STATEMENT

Data available on request from the authors.

ORCID

Annemarie Weissenbacher https://orcid.org/0000-0002-0582-1815
Rutger J. Ploeg https://orcid.org/0000-0001-7801-665X

REFERENCES

1. Sigdel TK, Lee S, Sarwal MM. Profiling the proteome in renal transplantation. *Proteomics Clin Appl*. 2011;5(5–6):269-280.
2. Sigdel TK, Salomonis N, Nicora CD, et al. The identification of novel potential injury mechanisms and candidate biomarkers in renal allograft rejection by quantitative proteomics. *Mol Cell Proteomics MCP*. 2014;13(2):621-631.
3. Marx D, Metzger J, Olagne J, et al. Proteomics in Kidney Allograft Transplantation-Application of molecular pathway analysis for kidney allograft disease phenotypic biomarker selection. *Proteomics Clin Appl*. 2019;13(2):e1800091.
4. Eikmans M, Gielis EM, Ledeganck KJ, Yang J, Abramowicz D, Claas FFJ. Non-invasive biomarkers of acute rejection in kidney transplantation: novel targets and strategies. *Front Med*. 2018;5:358.
5. Hricik DE, Nickerson P, Formica RN, et al. Multicenter validation of urinary CXCL9 as a risk-stratifying biomarker for kidney transplant injury. *Am J Transplant*. 2013;13:2634-2644.
6. Kaisar M, van Dullemen L, Charles P, et al. Subclinical changes in deceased donor kidney proteomes are associated with 12-month allograft function posttransplantation—a preliminary study. *Transplantation*. 2019;103(2):323-328.
7. Perco P, Heinzel A, Leierer J, et al. Validation of systems biology derived molecular markers of renal donor organ status associated with long term allograft function. *Sci Rep*. 2018;8:6974.
8. Kirita Y, Chang-Panesso M, Humphreys BD. Recent insights into kidney injury and repair from transcriptomic analyses. *Nephron*. 2019;143(3):162-165.
9. Weissenbacher A, Lo Faro L, Boubriak O, et al. Twenty-four-hour normothermic perfusion of discarded human kidneys with urine recirculation. *Am J Transplant*. 2019;19:178-192.
10. Weissenbacher A, Voyce D, Ceresa CDL, et al. Urine recirculation improves hemodynamics and enhances function in normothermic kidney perfusion. *Transplant Direct*. 2020;6(4):e541.
11. Weissenbacher A. *Normothermic kidney preservation*. University of Oxford; 2018.
12. Hosgood SA, Nicholson ML. The first clinical case of intermediate ex vivo normothermic perfusion in renal transplantation. *Am J Transplant*. 2014;14(7):1690-1692.
13. Hosgood SA, Saeb-Parsy K, Wilson C, Callaghan C, Collett D, Nicholson ML. Protocol of a randomised controlled, open-label trial of ex vivo normothermic perfusion versus static cold storage in donation after circulatory death renal transplantation. *BMJ Open*. 2017;7(1):e012237.
14. Kaths JM, Hamar M, Echeverri J, et al. Normothermic ex vivo kidney perfusion for graft quality assessment prior to transplantation. *Am J Transplant*. 2018;18:580-589.
15. Kaths JM, Cen JY, Chun YM, et al. Continuous normothermic ex vivo kidney perfusion is superior to brief normothermic perfusion following static cold storage in donation after circulatory death pig kidney transplantation. *Am J Transplant*. 2017;17:957-969.
16. Katane M, Ariyoshi M, Tateishi S, et al. Structural and enzymatic properties of mammalian d-glutamate cyclase. *Arch Biochem Biophys*. 2018;654:10-18.
17. Satou R, Shao W, Navar LG. Role of stimulated intrarenal angiotensinogen in hypertension. *Ther Adv Cardiovasc Dis*. 2015;9(4):181-190.
18. Bellomo R. Bench-to-bedside review: Lactate and the kidney. *Crit Care*. 2002;6:322-326.
19. Bartlett S, Espinal J, Janssens P, Ross BD. The influence of renal function on lactate and glucose metabolism. *Biochem J*. 1984;219(1):73-78.
20. Huang H, van Dullemen LFA, Akhtar MZ, et al. Proteo-metabolomics reveals compensation between ischemic and non-injured contralateral kidneys after reperfusion. *Sci Rep*. 2018;8(1):8539.
21. Tyanova S, Temu T, Cox J. The MaxQuant computational platform for mass spectrometry-based shotgun proteomics. *Nat Protoc*. 2016;11(12):2301-2319.
22. Szklarczyk D, Gable AL, Lyon D, et al. STRING v11: protein–protein association networks with increased coverage, supporting functional discovery in genome-wide experimental datasets. *Nucleic Acids Res*. 2019;47:D607-D613.
23. Perseus. http://www.biochem.mpg.de/5111810/Perseus Accessed August 25, 2020.
24. Hosgood SA, Nicholson ML. First in man renal transplantation after ex vivo normothermic perfusion. *Transplantation*. 2011;92(7):735-738.
25. Hosgood SA, Thompson E, Moore T, Wilson CH, Nicholson ML. Normothermic machine perfusion for the assessment and transplantation of declined human kidneys from donation after circulatory death donors. *Br J Surg*. 2018;105(4):388-394.
26. Hosgood SA, Nicholson ML. Ex vivo normothermic perfusion of declined human kidneys after inadequate in situ perfusion. *Am J Transplant*. 2014;14(2):490-491.

27. Kaths JM, Echeverri J, Linares I, et al. Normothermic ex vivo kidney perfusion following static cold storage-brief, intermediate, or prolonged perfusion for optimal renal graft reconditioning? *Am J Transplant*. 2017;17(10):2580-2590.
28. Kaths JM, Echeverri J, Goldaracena N, et al. Eight-Hour continuous normothermic ex vivo kidney perfusion is a safe preservation technique for kidney transplantation: a new opportunity for the storage, assessment, and repair of kidney grafts. *Transplantation*. 2016;100(9):1862-1870.
29. Urbanellis P, Hamar M, Kaths JM, et al. Normothermic ex-vivo kidney perfusion improves early DCD graft function compared to hypothermic machine perfusion and static cold storage. *Transplantation*. 2020;104:947-955.
30. Seong S-Y, Matzinger P. Hydrophobicity: an ancient damage-associated molecular pattern that initiates innate immune responses. *Nat Rev Immunol*. 2004;4(6):469-478.
31. Chouchani ET, Pell VR, Gaude E, et al. Ischaemic accumulation of succinate controls reperfusion injury through mitochondrial ROS. *Nature*. 2014;515(7527):431-435.
32. Martin JL, Gruszczyk AV, Beach TE, Murphy MP, Saeb-Parsy K. Mitochondrial mechanisms and therapeutics in ischaemia reperfusion injury. *Pediatr Nephrol*. 2019;34:1167-1174.
33. Reference GH.AGT gene. Genetics Home Reference. https://ghr.nlm.nih.gov/gene/AGTAccessed August 25, 2020.
34. UniProt. https://www.UniProt.org/ Accessed August 25, 2020.
35. STRING: functional protein association networks. https://string-db.org/cgi/input.pl Accessed August 25, 2020.
36. Carbonic anhydrase. In: Wikipedia. 2018. Accessed August 25, 2020.
37. Hui S, Ghergurovich JM, Morscher RJ, et al. Glucose feeds the TCA cycle via circulating lactate. *Nature*. 2017;551(7678):115-118.
38. Chen S, Fu H, Wu S, et al. Tenascin-C protects against acute kidney injury by recruiting Wnt ligands. *Kidney Int*. 2019;95(1):62-74.

SUPPORTING INFORMATION

Additional supporting information may be found online in the Supporting Information section.

How to cite this article: Weissenbacher A, Huang H, Surik T, et al. Urine recirculation prolongs normothermic kidney perfusion via more optimal metabolic homeostasis—a proteomics study. *Am J Transplant*. 2021;21:1740–1753. https://doi.org/10.1111/ajt.16334